Fluorescence Study of the Multiple Binding Equilibria of the Galactose Repressor†

Ke Wang,‡,§ Michael E. Rodgers,|| Dmitri Toptygin,|| Victor A. Munsen,|| and Ludwig Brand*,||

Department of Chemistry and Department of Biology, The Johns Hopkins University, Baltimore, Maryland 21218

Received August 12, 1997; Revised Manuscript Received October 31, 1997⊗

ABSTRACT: A fluorescence assay has been developed to study the multiple linked equilibria which function in regulation of the *Escherichia coli* galactose operon. Fluorescein 5-isothiocyanate was attached to Amino-Modifier C6dT at different positions in an oligonucleotide containing the sequence for the O_E site of the galactose operon. These fluorescently labeled oligonucleotides were used to study O_EDNA−GalR−D-galactose interactions. The data were analyzed and fit to various models including the classical competitive binding model as well as models involving the formation of a ternary DNA−repressor−inducer complex. Examination of the reduced χ-square of the various fits and comparison of fitted parameters with those obtained in independent experiments were used to distinguish different models. Since the ternary complex is likely to exist under physiological conditions, our results suggest that obligatory dissociation of GalR from DNA may not be required for induction of the *gal* operon. Rather, induction may involve the formation of a ternary complex of O_EDNA with GalR and D-galactose with a different conformation than the GalR−O_EDNA binary repressor complex.

Regulatory proteins control the process of transcription by binding to recognition sequences on DNA. Initiation of gene transcription in the galactose (*gal*) operon is repressed by the galactose repressor−DNA interaction (*1*, *2*). The *gal* operon of *Escherichia coli* contains two operator sites, O_E[1] and O_I, which are separated by 114 base pairs (*3*−*6*). The *E. coli* galactose repressor (GalR), the product of an unlinked gene (*galR*), is a dimer with a subunit molecular weight of 37 000. It inhibits the expression of the *gal* operon by binding to the two separated operator sites, O_E and O_I (*3*−*5*, *7*−*10*). Complete repression of the operon requires binding of GalR at both O_E and O_I sites, supercoiled DNA, and binding of the histone-like protein HU (*11*). Binding of the Gal repressor to the *gal* operator sites is inhibited by D-galactose and D-fucose, which are inducers of the operon (*4*, *7*−*10*).

The consensus half-symmetry sequence of the homologous regions of both O_E and O_I is 5′ GTG(G/T)AANC (*4*, *5*). Ten of 16 base pairs of the homologous regions of O_E and O_I are identical, and O_E has better dyad symmetry than O_I (*3*−*5*). Each half-symmetry sequence binds to one subunit of Gal repressor dimer (*4*, *5*). Gel mobility shift assays have been used to characterize the Gal repressor−DNA interaction and the effect of D-galactose on the binding of GalR to DNA (*4*, *6*, *9*, *12*, *13*).

Fluorescence methods have been developed as a complementary approach to characterize the equilibrium binding of DNA to specific binding proteins without separation of free and bound species, *i.e.*, under true solution conditions (*14*−*27*). Attachment of a fluorescent probe on DNA is often required for fluorescence studies of DNA−protein interactions. Fluorescence probes have been attached both to the 5′-termini (*23*−*26*, *28*−*36*) and to modified bases in internal positions of oligonucleotides (*14*, *15*, *18*, *20*, *21*, *37*). For attachment of a fluorescent probe to an internal position of the recognition sequences, a modified base with a linker arm terminating in a reactive group such as a primary amine must be introduced directly into oligonucleotides by DNA synthesizers. Amino-Modifier C2dT and Amino-Modifier C6dT are commercially available modified bases used to replace thymidine residues. After incorporation into oligonucleotides and subsequent deprotection of the primary amine group, the modified base can be labeled with an appropriate fluorescent dye. The formation of a complex between labeled DNA and a specific binding protein may be monitored by a change of the anisotropy and/or intensity of the extrinsic fluorophore (*14*, *15*, *20*−*22*, *24*−*26*).

The long-range aim of these studies is to better understand both the molecular events and time-dependent changes involved in the regulation of DNA function. As a first step, it is important to define the thermodynamic intermediates in this process. It is advantageous to do this in dilute solution under a variety of conditions. In this study, we present a fluorescence-based approach to characterize some of the multiple linked equilibria which function in the transcription regulation of the *E. coli* galactose operon. Fluorescein has been attached to an Amino-Modifier C6dT nucleotide

† Supported by NIH Grant GM-11632.

* Author to whom correspondence should be addressed.

‡ Department of Chemistry.

§ Portions of this work will be submitted to the Johns Hopkins University in partial fulfillment of the requirements for the degree of Ph.D.

|| Department of Biology.

⊗ Abstract published in *Advance ACS Abstracts,* December 15, 1997.

[1] Abbreviations: FITC, fluorescein 5-isothiocyanate (isomer I); HPLC, high-pressure liquid chromatography; bp, base pair; Amino-Modifier C6dT, 5′-dimethoxytrityl-5-[*N*-(trifluoroacetylaminohexyl)-3-acrylimido]-2′-deoxyuridine,3′-[(2-cyanoethyl)-(*N*,*N*-diisopropyl)]-phosphoramidite; O_E, external operator binding site in the *E. coli* galactose operon; O_I, internal operator binding site in the *E. coli* galactose operon; GalR, *E. coli* galactose repressor protein.

S0006-2960(97)02004-7 CCC: $15.00 © 1998 American Chemical Society
Published on Web 01/06/1998

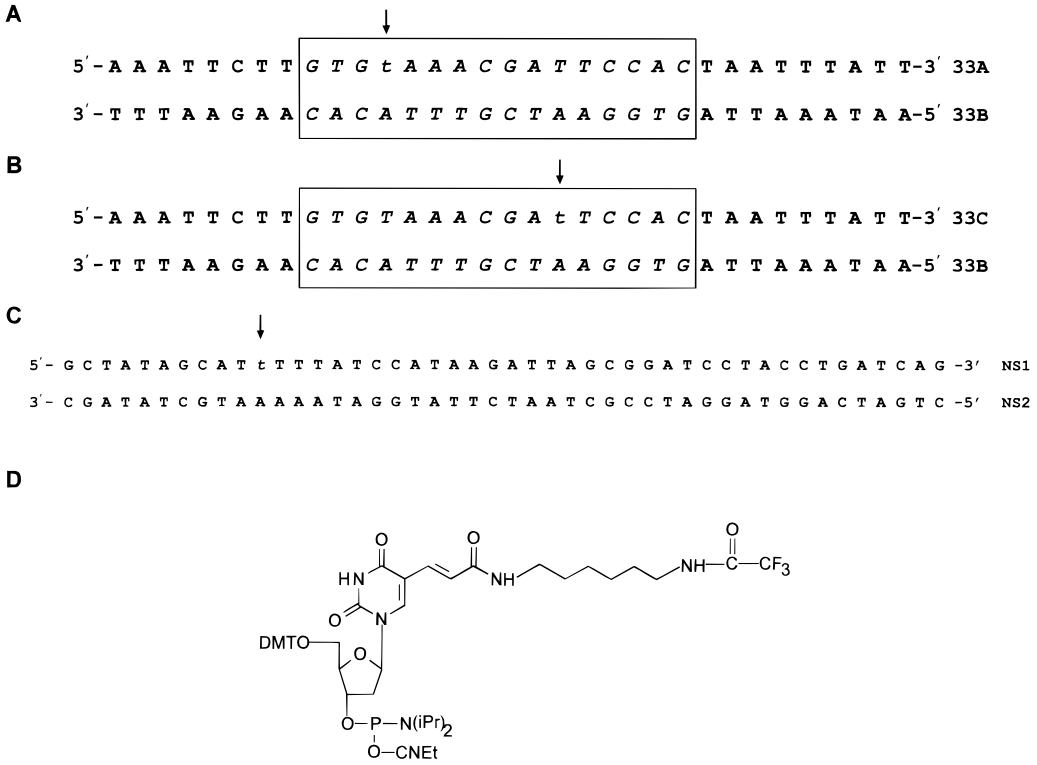

FIGURE 1: Sequence of the various oligonucleotides used in this study. Lower case *t* indicates a modified base at positions indicated by arrows. The boxes indicate the position of the *gal* O_E site within the oligonucleotides. (A) O_EDNA with modified base at position 12; (B) O_EDNA with modified base at position 19; (C) nonspecific control DNA with modified base at position 11; (D) Structure of Amino-Modifier C6dT.

incorporated at two different positions in an oligonucleotide containing the O_E site of the *gal* operon. These labeled DNAs are used to characterize the O_EDNA−GalR−D-galactose interactions. Various models are used to analyze and fit the data. Examination of the reduced χ-square of the various fits and comparison of fitted parameters with those obtained in independent experiments are used to distinguish different models. It will now be possible to make use of the same spectroscopic signals to investigate kinetic aspects of this regulatory mechanism.

MATERIALS AND METHODS

Materials. 33 base oligonucleotides containing the O_E site of the *gal* operon (33A, 33B, and 33C) and 46 base control oligonucleotides (NS1 and NS2) were obtained in HPLC-purified forms from Integrated DNA Technologies, Inc. (Coralville, IA). The 33 base complementary oligonucleotide (33B) was also obtained in HPLC-purified form from CyberSyn (Lenni, PA). The sequences are shown in Figure 1A−C. The italicized, boxed segments indicate the homologous region to the O_E site (33A/33B and 33C/33B). The lower case "*t*" denotes an Amino-Modifier C6dT which replaces a thymidine base. Its structure is shown in Figure 1D. This modified base is labeled with FITC as described below. The control DNA contains the *araI* site of the *araBAD* operon (*38*).

FITC (fluorescein 5-isothiocyanate, isomer I) was purchased from Molecular Probes. D-Galactose was obtained from Pfanstiehl Laboratories, Inc. HPLC-grade solvents were purchased from J. T. Baker Inc. and Fisher Scientific Inc. All other chemicals are reagent grade or better.

FITC-Labeling. The 33-mer containing a modified base (33A or 33C) was dissolved in 0.2 M Na_2CO_3−$NaHCO_3$ (pH 10) to yield a final concentration of 1 mM unlabeled 33-mer; 100 mg/mL FITC (isomer I) (257 mM) dissolved in dimethylformamide was added to the unlabeled oligonucleotide at a 50:1 molar ratio. The reaction was performed at room temperature in the dark. After 4 h, a second aliquot of 257 mM FITC solution was added to give the final molar ratio of FITC to the unlabeled 33-mer of 100:1, and the reaction was allowed to proceed overnight (∼20 h). The reaction mixture was passed through a Sephadex G-25 column in 0.1 M triethylamine acetate, pH 7.0, to remove the excess unreacted FITC. The eluted oligonucleotides were applied to a reverse phase C18 column to separate fluorescein-labeled 33-mer from unlabeled 33-mer. Samples were eluted at a flow rate of 1 mL·min^{-1} with the following program: (1) 4 min isocratic elution with solvent A (0.1 M triethylamine acetate, 10% acetonitrile, pH 7.0); (2) 1% min^{-1} increase in solvent B (acetonitrile) for 8 min (8% B, final); (3) 0.5% min^{-1} increase in solvent B for 34 min (25% B, final); (4) gradient increase in solvent B to 100% over 4 min; (5) 10 min isocratic elution with solvent B. The eluted fluorescein-labeled 33-mer was collected and lyophilized. The fluorescein-labeled 46 base control oligonucleotide was prepared by the same method.

Formation of Fluorescent Duplexes. The fluorescein-labeled single-strand oligonucleotide and its complementary strand were dissolved in an experimental buffer containing 25 mM KH_2PO_4−K_2HPO_4, pH 7.4, 300 mM KCl, 1 mM $MgCl_2$, and 0.02% (w/v) NaN_3, and their concentrations were determined by absorption spectroscopy. The molar extinction coefficients of each oligonucleotide were calculated from sequences of related oligonucleotides (*39*), and the values are as follows: 33A and 33C, $\epsilon_{260} = 3.709 \times 10^5$ M^{-1} cm^{-1}; 33B, $\epsilon_{260} = 3.977 \times 10^5$ M^{-1} cm^{-1}; NS1, $\epsilon_{260} = 5.068 \times$

10^5 M^{-1} cm^{-1}; NS2, $\epsilon_{260} = 5.276 \times 10^5$ M^{-1} cm^{-1}. No corrections were made for the Amino-Modifier C6dT or for the absorption of fluorescein at 260 nm (*21*). A slight molar excess of complementary strand was mixed with the fluorescein-labeled single strand, and duplexes were annealed by incubation at 90 °C for 10 min followed by slow cooling to room temperature over 3 h.

GalR. GalR was expressed in *E. coli* BL21(DE3) transformed with either pSA-401 or pET-GalR (plasmids containing the GalR structural gene downstream from a T7 promoter). pSA-401 (*40*) was kindly provided by S. Adhya. pET-GalR (manuscript in preparation) is a streamlined construct containing *galR* in a pET-11d expression vector. GalR was purified by a modification of the method of Majumdar *et al*. (*9*) (manuscript in preparation). The GalR used in this study was better than 95% pure as judged by densitometry of Coomassie blue stained SDS−polyacrylamide gels of normal and overloaded GalR samples. It was also found to be better than 97% pure by reverse phase HPLC. Following purification, GalR was dialyzed into buffer [25 mM KH_2PO_4−K_2HPO_4, pH 7.4, 300 mM KCl, 1 mM $MgCl_2$, and 0.02% (w/v) NaN_3] for the gel mobility shift assays or into buffer [25 mM KH_2PO_4−K_2HPO_4, pH 7.4, 1 M KCl, 5% glycerol, 1 mM $MgCl_2$, and 0.02% (w/v) NaN_3] for fluorescence measurements of GalR binding to labeled DNA. High salt and glycerol were included to enhance the solubility of GalR. The concentration of GalR was determined by absorption measurements assuming a molar extinction coefficient = 39 600 M^{-1} cm^{-1} at 280 nm for the GalR dimer (*6*).

It is important to consider the competency of GalR both in DNA and in inducer binding. In all calculations, we have assumed 100% competency in both DNA and inducer binding. Lower levels of competency will affect the absolute values of our estimated binding parameters but will not alter the basic conclusions of this study.

Previous studies using a similar preparative method found approximately 40−50% of GalR to be DNA binding competent (*6*). We have performed gel shift assays on mixtures of GalR with excess O_EDNA and quantitated the amount of GalR remaining unbound using a silver stain detection system. Using this method, we estimate the fraction of DNA binding competent GalR to be at least 70%. Quantitative analysis using silver stain systems has many technical difficulties, and we are working to improve this method and our estimate of viable GalR.

We have no absolute assessment of D-galactose binding competency; however, a D-galactose-dependent binding step is part of the purification (manuscript in preparation). Further, when assaying D-galactose binding of different GalR preparations using intrinsic tryptophan fluorescence, we find a highly reproducible 23% intensity enhancement at saturating inducer concentrations.

Absorbance Spectroscopy and HPLC. Absorbance measurements were made using a Shimadzu spectrophotometer (Model UV160/CL750) interfaced to a computer for data acquisition. HPLC was performed on a Varian Model 5000 liquid chromatograph equipped with an UV-50 detector. A Beckman Ultrasphere ODS 5 μm column (4.6 mm × 25 cm) was used for all separations. The detector output was recorded on a BD40 recorder (Kipp & Zonen), and fractions were collected on a Frac-100 fraction collector (Pharmacia).

Gel Studies. Native polyacrylamide gel electrophoresis was used to initially characterize fluorescein-labeled single-strand oligonucleotides, complementary strands, labeled DNA, and binding of GalR to labeled O_EDNA. For analysis of oligonucleotides and DNA, 12 pmol of each sample was mixed with one-fifth volume of a loading buffer containing 15% ficoll, 0.25% (w/v) bromophenol blue, and 0.25% (w/v) xylene cyanol. The mixtures were loaded on a 20% polyacrylamide [acrylamide:*N*,*N*′-methylenebis(acrylamide) ratio of 38:2] gel and run at 100 V for 3 h. Running buffer (TBE) was continuously circulated throughout the run. Following electrophoresis, the gel was illuminated on a UV light box and photographed through a KV 470 filter to monitor the emission due to fluorescein. After subsequent staining with ethidium bromide, the gel was rephotographed through a Corning CS3-70 filter to monitor total DNA.

For gel mobility shift assays, 6 pmol of labeled DNA was mixed with GalR at DNA:GalR molar ratios equal to 1:2 and 1:5 (concentrations were 0.7 mM:1.4 mM and 0.3 mM:1.5 mM, respectively). All samples were in a solution containing 300 mM KCl, 25 mM KH_2PO_4−K_2HPO_4, pH 7.4, 1 mM $MgCl_2$, and 0.02% (w/v) NaN_3. Samples were mixed with loading buffer as above, loaded on a 15% polyacrylamide [acrylamide:*N*,*N*′-methylenebis(acrylamide) 150:1] gel, and run at 100 V. The running buffer was circulated throughout the run. After 1.5−2 h of electrophoresis, the gel was photographed as described above.

Steady-State Fluorescence Anisotropy and Intensity Studies. All steady-state anisotropy and intensity data were recorded on a SLM 48000 spectrofluorometer configured in the T format. The excitation wavelength was 495 nm, and the excitation slit widths were 4 nm. A Corning 493 nm cutoff filter (cs 3-69) was used in the emission beam while recording all fluorescence anisotropy and intensity data. The temperature was controlled at 25 °C by a Neslab circulating temperature bath, and samples were continuously stirred by a magnetic stirrer.

A 2.7 mL sample of 90 nM DNA was titrated by the addition of small volumes of stock GalR. Subsequently, the mixture of DNA and GalR was titrated with D-galactose. After each addition of GalR or D-galactose, the solution was allowed to equilibrate at least 2 min. Anisotropy readings were found to be stable after this time. DNA and D-galactose samples were in a buffer containing 25 mM KH_2PO_4−K_2HPO_4, pH 7.4, 0.3 M KCl, 1 mM $MgCl_2$, and 0.02% (w/v) NaN_3. The stock GalR used for these titrations was dialyzed into 25 mM KH_2PO_4−K_2HPO_4, pH 7.4, 1 mM $MgCl_2$, 0.02% NaN_3, and either 0.3 M KCl or 1 M KCl and 5% glycerol. The low KCl samples were used for the initial low [GalR] points in these titrations. In separate experiments, titrations of labeled O_EDNA were carried out with the mixtures of GalR and D-galactose at various fixed molar ratios. Such titrations were used to better define the binding surface as discussed later.

Data Analysis. The raw data collected in all titrations were steady-state fluorescence anisotropy and total fluorescence intensity. In these experiments, anisotropy is the only spectral response which contains significant information since intensity changes were relatively small. Because anisotropy is not a linear spectroscopic response, the raw data were recast as two linear response components prior to analysis: I_0, the total intensity, and $r \cdot I_0$, the product of the total

intensity and the anisotropy. In terms of the polarized components of intensity, $I_{||}$ and $I_{\perp}$, these are given by

$$I_0 = I_{||} + 2GI_{\perp} \text{ and } r \cdot I_0 = I_{||} - GI_{\perp}$$

where G is a factor that corrects for differences in the sensitivity of the instrument to vertically and horizontally polarized light. All binding data were fitted using the program SPECTRABIND (*41*). The assumed standard deviations were 0.001 for anisotropies and 1% of the value for total intensities. For the concentrations of the three chemical components, DNA, GalR, and D-galactose, relative standard deviations were assumed to be 1%. Different models which include the various postulated linked binding equilibria were used to simultaneously fit the anisotropy and intensity data and to extract binding constants and their confidence intervals.

In the analysis below, the estimated parameters for binary complexes are well-defined by the titrations. Since we are dealing with a system that has essentially one spectroscopic response, the binding constants associated with the postulated ternary complexes are very sensitive to systematic errors in concentrations. Such errors will not be reflected in either χ^2 or the estimated confidence intervals. Much of the information for parameter estimation comes from the chemical data, and the accuracy of these concentrations is very important. At the present time, we have no way of distinguishing between systematic errors and changes in fitting parameters. We are encouraged by the fact that repeated titrations on identical samples are quite reproducible.

RESULTS

Labeling and Purification of Oligonucleotides. Oligonucleotides containing the modified bases were labeled according to the procedure described under Materials and Methods. The fluorescein-labeled 33-mer was separated from the unlabeled 33-mer on a reverse-phase HPLC column. The retention times of labeled and unlabeled 33 base single-stranded oligomers are approximately 19 and 15 min, respectively, with base line separation between. The labeled 33-mer at position 19 and labeled 46-mer were prepared and purified in the same manner (data not shown).

Annealing and Native PAGE. For each oligonucleotide, the fluorescein-labeled single strand was mixed with a slight molar excess of complementary strand to assure that no labeled single strand was present after annealing. Samples were annealed as described above, and a native 20% polyacrylamide gel was used to characterize the labeled single strand, the complementary strand, and the annealed labeled DNA. Results are shown in Figure 2 for oligonucleotides 33A and 33B. Both single-strand oligonucleotides migrate as single bands on the native gel. The electrophoretic mobility of the fluorescein-labeled single-strand oligonucleotide is slightly reduced compared with the complementary strand. The labeled double-stranded DNA shows a single band when monitoring the emission of fluorescein attached on the DNA (Figure 2A) but shows two separate bands when stained with ethidium bromide (Figure 2B). The more intense, upper band corresponds to the fluorescein-labeled DNA while the less intense, lower band shows no fluorescein signal. This result indicates that some fluorescein comes off the oligonucleotides during the annealing procedure. Similar results were obtained for the other oligonucleotides.

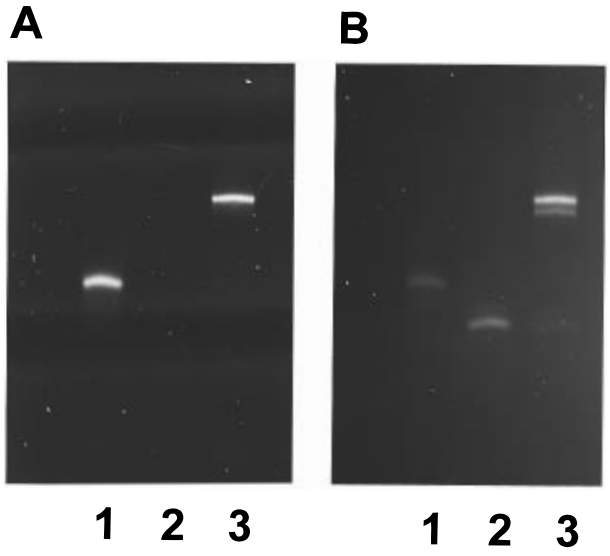

FIGURE 2: Characterization of fluorescein-labeled oligonucleotides, complementary strand oligonucleotides, and fluorescein-labeled duplexes. 12 pmol of oligonucleotides and duplexes was used. Lane 1 is fluorescein-labeled 33A; lane 2 is 33B; lane 3 is fluorescein-labeled (33A/33B) DNA. (A) Gel photographed through a KV 470 filter using UV illumination to monitor the fluorescein emission; (B) gel photographed using UV illumination after staining with ethidium bromide.

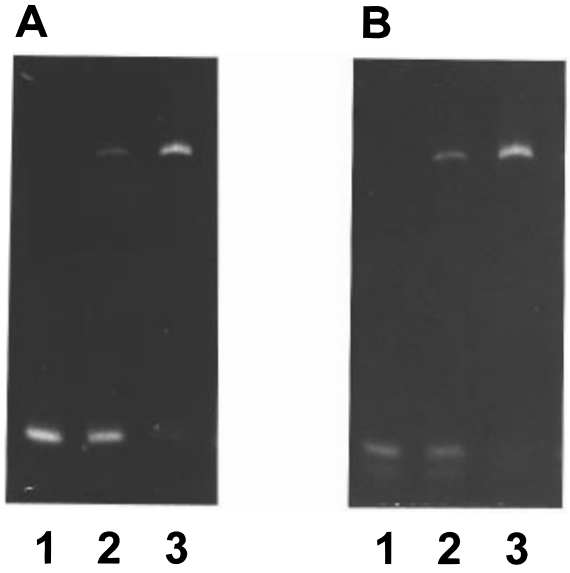

FIGURE 3: Gel mobility shift assay of the binding of fluorescein-labeled 33A/33B duplexes to GalR. Each lane contains 6 pmol of DNA. Lane 1 is fluorescein-labeled DNA, loading volume = 6 μL; lane 2 contains labeled DNA and GalR at 1:2 molar ratio, loading volume = 9 μL; and lane 3 contains labeled DNA and GalR at 1:5 molar ratio, loading volume = 21.5 μL. (A) Gel photographed through a KV 470 filter using UV illumination to monitor the fluorescein emission; (B) picture photographed using UV illumination after staining with ethidium bromide.

DNA−GalR Interaction Characterized by the Gel Mobility Shift Assay. Figure 3 shows the significant decrease in electrophoretic mobility of labeled F-12-O_EDNA in the presence of increasing amounts of GalR. The result indicates that GalR binds to labeled O_EDNA in a typical fashion.

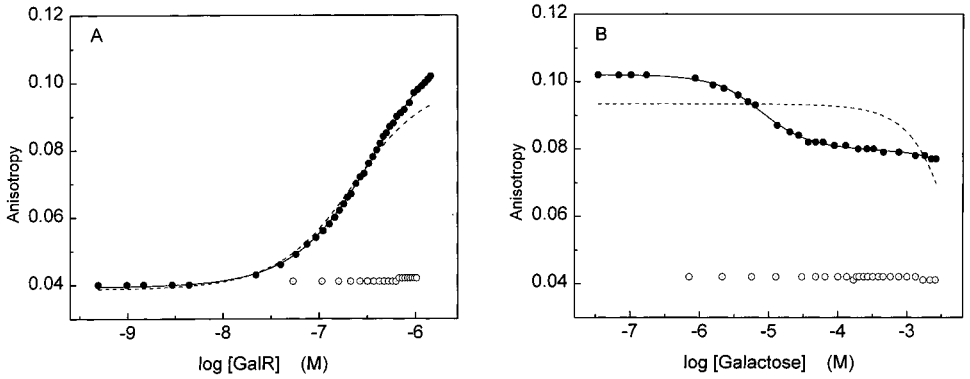

FIGURE 4: Titration of F-19-O_EDNA with GalR using steady-state fluorescence anisotropy (A) and back-titration of the mixture with D-galactose (B). The titration of fluorescein-labeled nonspecific DNA with GalR is also shown as (⊙) in panel A, and the continued titration with D-galactose is shown as (⊙) in panel B. Total intensity data were simultaneously collected (not shown), and both intensity and anisotropy were used in the fitting. The initial DNA concentration was 90 nM. The buffer contained 25 mM KH_2PO_4/K_2HPO_4 (pH 7.4), 300 mM KCl, 1 mM $MgCl_2$, and 0.02% NaN_3, and the temperature was 25 °C. Excitation and emission settings are described in Materials and Methods. Two models, a binary model and a ternary model, were used to analyze all data and subsequently to generate the fit curves. The dashed line (---) is the fitted curve from the binary model, and the solid line (—) shows the best-fit curve to the ternary model.

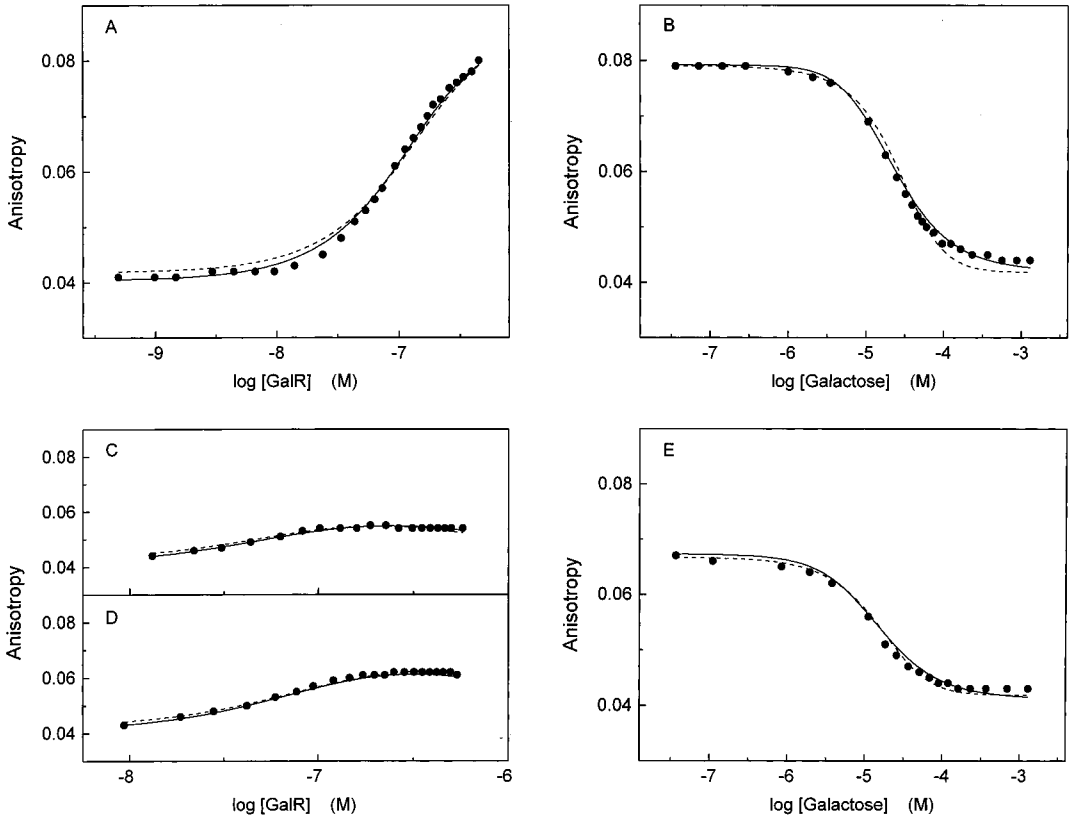

FIGURE 5: Titration of F-12-O_EDNA with GalR using steady-state fluorescence anisotropy (A); back-titration of the mixture with D-galactose (B); titrations of F-12-O_EDNA with mixtures of GalR and D-galactose at molar ratios of 1:100 (C) and 1:50 (D); and titration with D-galactose of a mixture of GalR and F-12-O_EDNA at a fixed molar ratio of 1.68:1 (E). Total intensity data (not shown) were also collected and used in the fitting. Experimental conditions were the same as those in figure 4. A ternary model and a binary model were used to analyze all data and subsequently to generate the fitted curves. The dashed line (---) is the fitted curve from the binary model, and the solid line (—) shows the fitted curve from the ternary model.

O_EDNA−GalR−D-Galactose Interactions Characterized by Fluorescence Spectroscopy. Steady-state fluorescence anisotropy and intensity of fluorescein-labeled O_EDNA were used to monitor the formation of the O_EDNA−GalR complex during titrations of O_EDNA with GalR (Figures 4A and 5A). Subsequent titrations of the resultant mixtures with D-galactose were used to monitor the effect of D-galactose on the O_EDNA−GalR complex (Figures 4B and 5B).

The titration of F-19-O_EDNA with GalR shows that the steady-state fluorescein emission anisotropy increases from 0.040 (free DNA) to 0.102 with the addition of GalR to 1.44 μM (Figure 4A, close circles). Subsequent titration of the above mixture with D-galactose shows a decrease in steady-state fluorescein anisotropy from 0.102 to 0.077 with increasing concentration of D-galactose to 2.63 mM (Figure 4B, close circles). After correction for dilution, there is almost no change in fluorescence intensity during these titrations ($<\pm 2\%$, data not shown). In control experiments, similar titrations of fluorescein-labeled nonspecific DNA (F-11-NS_DNA) with GalR show essentially no change in

anisotropy with increasing concentration of GalR (Figure 4A, open circles) or in subsequent titration with D-galactose (Figure 4B, open circles)

Attachment of the label to a different position within the O_EDNA led to somewhat different titration results. The steady-state anisotropy of F-12-O_EDNA titrated with GalR shows an enhancement from 0.041 (free DNA) to 0.080 when the GalR concentration increases to 0.45 μM (Figure 5A). The back-titration of the mixture with D-galactose to a final concentration of 1.3 mM leads to a drop in the fluorescence anisotropy of the system to 0.044 (Figure 5B), a value that is only slightly higher than the initial anisotropy of free DNA (0.041). There is a small increase (<7% after the correction of the dilution effect) in fluorescence intensity when F-12-O_EDNA is titrated with GalR and the back-titration with D-galactose shows a decrease in fluorescein intensity. Results show that the up-titrations of DNA with GalR and the back-titrations with D-galactose are significantly different when fluorescein is labeled at two different positions.

Fluorescence anisotropy and intensity titrations of F-12-O_EDNA with the mixtures of GalR and D-galactose at molar ratios of 1:100 and 1:50 were also carried out (Figures 5C,D). As in the titration of F-12-O_EDNA above, the initial steady-state anisotropy was 0.041. Addition of the GalR−D-galactose mixture resulted in an increase in anisotropy to a peak value followed by a small progressive decrease as further protein and sugar were added. The peak values were 0.055 and 0.062 for mixture ratios of 1:100 and 1:50, respectively. These are somewhat less than the maximum value of 0.08 seen above (Figures 5A,B). The final result shows the titration of a mixture of GalR and F-12-O_EDNA with D-galactose (Figure 5E). This is similar to the experiment depicted in Figure 5B except the GalR:F-12-O_EDNA ratio was 1:1.68. As discussed below, the last three titrations provide additional data over the binding surface which aid in distinguishing binding models and estimating the equilibrium binding parameters.

DISCUSSION

The fluorescence assay described in this paper shows that modified deoxyuridine can be used to replace thymidine residues at desired positions in the operator site of the *gal* operon and can be labeled with an appropriate fluorescent dye such as fluorescein. The interaction of *gal* repressor with fluorescently labeled DNA containing the regulatory binding sequence of the operator site of the *gal* operon was investigated by measuring changes of steady-state fluorescence anisotropy and intensity of the labeled DNA upon addition of repressor protein. The effect of inducer, D-galactose, on the labeled DNA−*gal* repressor complex has also been studied by monitoring fluorescence changes. This method allows direct determination of the equilibrium binding constants of multiple linked equilibria under true solution conditions, without separation of free and bound species, and can readily be used to study the effects of various solution conditions such as salt concentration, ligand concentration, pH, and temperature on the binding equilibria.

Design of the Oligonucleotides. The oligonucleotides used in this study contain 7 and 8 bp flanking regions on either side of the 16 bp *gal* O_E consensus sequence. These are included as they may be needed to increase the binding ability to *gal* repressor. DNase I and dimethyl sulfate protection studies show repressor protection of about 3 bases on either side of the binding box and protection on the upstream side of O_E may be as much as 6 bases (*5*, *6*). In the case of TyrR, 10 bp of the wild-type flanking region on each side of the *tyr*R operator sequence was required to detect binding using a gel mobility shift assay (*15*). We have used a modified deoxyuridine at specific positions to attach labels to DNA. These modified bases, such as the Amino-Modifier C6dT, contain a linker arm attached to the 5 position of uracil. In the B-DNA conformation, the 5 position of pyrimidines faces outward from the major or minor grooves of the helix and is not involved in the base pair hydrogen bonding (*32*). Thus, substitution at the 5 positions of pyrimidines should not cause significant interference with base pairing nor any major distortion of the double helix structure (*42*). The effect of such substitutions on the interaction with DNA binding proteins is dependent on a number of factors and is discussed in more detail below.

Analysis of the Labeling Procedure. Characterization of the fluorescein-labeled double-stranded DNA on polyacrylamide gels shows a single band when monitoring the fluorescein emission but shows two bands after staining with ethidium bromide. The upper, more intense band and lower, less intense band correspond to fluorescein-labeled DNA and unlabeled DNA, respectively. Control experiments (data not shown) revealed that subjection of fluorescein-labeled single-strand oligonucleotide to annealing conditions also yielded one fluorescein-labeled band and two ethidium-stained bands. These results indicate that some fluorescein comes off the oligonucleotides during annealing. This loss of fluorescent label was unexpected, and its cause remains to be determined. The annealed DNA was used for all fluorescence measurements without further purification to remove unlabeled DNA. The concentration used in all analyses was calculated from the initial concentration of fluorescein-labeled single strand corrected for the volume change upon addition of complementary strand.

The fraction of DNA that has lost label is small, and we have included the total concentration of DNA in our analysis. In spectroscopic measurements, we see only labeled DNA; the presence of a second DNA species can complicate analysis under some conditions. If both labeled and unlabeled DNA have comparable binding characteristics, then it is appropriate to use the total concentration of DNA in the analysis, and there is no problem. In the case of F-12-O_E-DNA, this seems to be the case since our estimated K_d for GalR with labeled O_EDNA is comparable to that estimated for unlabeled O_EDNA by independent means (see below). On the other hand, if unlabeled DNA and labeled DNA bind GalR with different affinities, then an error in the estimated binding parameters will be introduced. The magnitude of this error will depend on experimental conditions and binding affinities. The estimated parameters are relatively insensitive to DNA concentration when it is less than K_d. In the case of F-19-O_EDNA, the K_d is >300 nM while the experimental concentration of O_EDNA is 90 nM. Thus, a small amount of unlabeled DNA with different binding properties will not significantly alter the concentration of free GalR in equilibrium with labeled DNA nor will the true concentration of labeled DNA markedly affect the analysis. Thus, under our

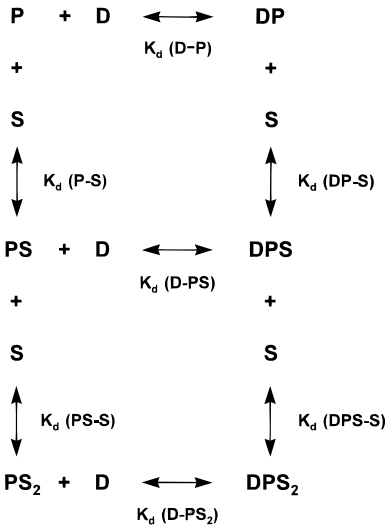

FIGURE 6: Complete linkage scheme for the multiple linked equilibria used to describe these data are shown. P represents GalR, D represents O_EDNA, and S indicates D-galactose. The binary model includes only free species and binary complexes: P, D, S, PD, PS, and PS_2. The ternary model includes all species shown above.

experimental conditions, the error in estimated parameters due to these factors will be small.

Analysis of the Binding Data. The program SPECTRABIND was used to simultaneously fit all anisotropy and intensity data by one of the two binding models, referred to as binary and ternary. The binary model corresponds to the classical competitive binding scheme for repressor−operator−inducer function. Recently, Chatterjee and co-workers (*43*) suggested a model which departs from the classical formalism. Their model involves four linked equilibria and includes the formation of a ternary complex of operator (O_EDNA)−repressor (GalR)−inducer (D-galactose). They conclude that the inducer may derepress transcription without dissociation of the repressor−operator complex. Since this model did not take into account the binding of two D-galactose molecules per GalR dimer, we have expanded the ternary model to include this equilibrium.

Both models assume two equal and independent binding sites of D-galactose to free GalR. The binary model assumes that GalR is unable to simultaneously bind DNA and D-galactose. The ternary model allows formation of two ternary complexes of O_EDNA, GalR, and D-galactose (DPS and DPS_2) with equal and independent binding of D-galactose to GalR in the O_EDNA−GalR complex. The complete linkage scheme corresponding to the ternary model is shown in Figure 6. This model considers all species and equilibria while the binary model excludes chemical species involving three chemical components (DNA, GalR, D-galactose) and the corresponding equilibria. The binary model has a total of six species and three linked equilibria while the ternary model comprises eight species and seven linked equilibria.

The simulated curves generated from the best-fit parameters of these models to our data are superimposed on the data in Figures 4 and 5. Table 1 summarizes the estimated dissociation constants, confidence intervals, and reduced χ^2's. The first indication that a competitive binding model was not applicable was the observation that the anisotropy of free F-19-O_EDNA was substantially lower than the mixture of GalR plus F-19-O_EDNA in the presence of a vast excess of D-galactose. This is borne out by the fitting results where the values of the reduced χ^2 of the binary model and ternary model are 13.6 and 0.11, respectively. It is clear from these results that the competitive binding, binary model does not adequately describe the data.

Table 1

equilibrium	binary model	ternary model
	F-19-O_EDNA Binding Constants[a]	
(D−P)	182 nM (175−189)	319 nM (306−332)
(P−S)	0.95 mM (0.91−0.99)	1.65 μM (1.04−2.61)
(PS−S)	3.80 mM	6.6 μM
(DP−S)		1.86 μM (1.31−2.65)
(DPS−S)		7.44 μM
(D−PS)		360 nM
($D-PS_2$)		406 nM
reduced χ^2	13.60	0.11
	F-12-O_EDNA Binding Constants[a]	
(D−P)	94.3 nM (87.8−101)	76.2 nM (70.2−82.6)
(P−S)	7.74 μM (7.47−8.01)	2.53 μM (2.26−2.84)
(PS−S)	30.96 μM	10.1 μM
(DP−S)		5.52 μM (4.93−6.17)
(DPS−S)		22.1 μM
(D−PS)		166 nM
($D-PS_2$)		363 nM
reduced χ^2	0.72	0.51

[a] Confidence intervals are shown in parentheses. Parameters without confidence intervals are not independent but are linked to the fitted parameters by the equilibrium equations.

For F-12-O_EDNA, the interpretation is not as straightforward. In this case, the anisotropy of F-12-O_EDNA is very close to that of GalR plus F-12-O_EDNA in the presence of a vast excess of D-galactose. There is, however, a small but reproducible difference (0.041 *vs* 0.044). Nevertheless, we were unable to find unique values of fitting parameters when fitting the two initial titrations by the ternary model (Figure 5A,B). If one assumes that the same binding model applies, independent of the labeling site, then additional titration data are needed for F-12-O_EDNA in order to have a unique χ^2 minimum with the ternary model. This additional data should cover a larger part of the equilibrium binding isotherm surface, and three supplemental titrations are shown in Figure 5C−E. The total equilibrium binding isotherm surface for F-12-O_EDNA is shown in Figure 7 along with the five titrations that were used to define it. This surface was generated using the parameters of the best fit of all data sets by the ternary model. The values of the reduced χ^2 for this fit and for the fit to the binary model are shown in Table 1. The ternary model reduced χ^2 is significantly better than that of the binary model, although the difference is not as dramatic as was the case for F-19-O_EDNA.

Interpretation of the Fluorescence Change. The fluorescence signals measured in this study are the steady-state anisotropy and steady-state fluorescence intensity of fluorescein-labeled oligonucleotides. Upon binding of GalR, a small enhancement (<7%) in fluorescence intensity is observed with F-12-O_EDNA while essentially no change (<2%) is observed with F-19-O_EDNA. In principle, the intensity change can only be due to the direct interaction of fluorescein with GalR and may be due to the following: a change of radiation rate, a change of radiationless rate, or a change of the molar extinction coefficient of the fluorophore. Further fluorescence lifetime and absorbance studies are needed to resolve these possibilities.

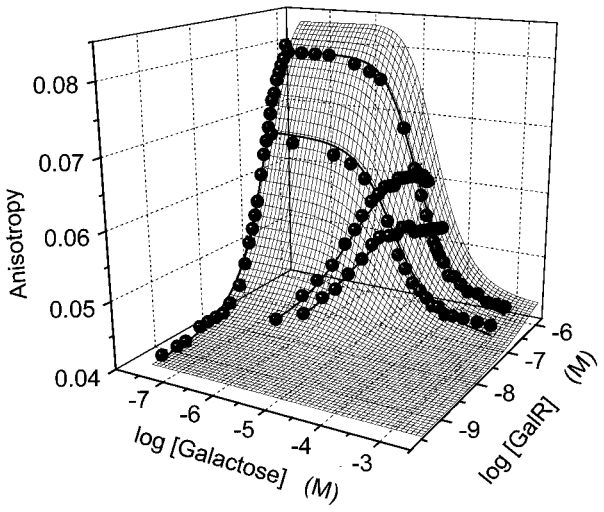

FIGURE 7: Total equilibrium binding isotherm surface for data obtained with F-12-O_EDNA is shown. The surface was generated using the ternary model with the best-fit parameters for this data set. Superimposed on the surface is the actual data. Since one cannot display zero values on a log scale, the titration of GalR into DNA in the absence of D-galactose is plotted at −7.5 on the log [D-galactose] scale. This plot shows that the binding surface is well sampled by the data as required for parameter estimation.

The anisotropy changes associated with the binding of the labeled oligonucleotides to GalR have their origin mainly in the rotational behavior of the fluorescein although, as indicated above, a change in the decay time may also have a role. The rotation of the fluorescein in the GalR bound species depends on the motion of the entire GalR−DNA complex but to a larger extent on segmental motions of the DNA binding domains, motions of the nucleotide fragments, and segmental motions of the fluorescein probe. The fluorescence anisotropy of a fluorescein-labeled 42 bp DNA with a relatively short linker arm described previously (*21*) was 0.10−0.13 as compared to 0.04 observed here. This suggests that the probe on the longer linker arm undergoes more local motion than is the case with the shorter linker arm. It is likely that the emission anisotropy is dominated by the local motion of the probe and that this local motion is different depending on the absence or presence of D-galactose on the GalR. The limiting emission anisotropy of labeled O_EDNA-GalR in the presence of saturating D-galactose is lower than that of the binary complex of O_E-DNA−GalR but larger than the value found with free O_E-DNA (Table 2). This provides evidence for a change in the local conformation at the DNA binding site induced by the binding of D-galactose. It is known that binding of D-galactose to GalR changes the conformation of GalR. Specifically, D-galactose binding causes enhancement in the intrinsic tryptophan fluorescence (*44*), enhanced solubility, altered thiol reactivity, and enhanced thermal stability (manuscript in preparation). Thus, it seems likely that D-galactose binding to the DNA−GalR complex results in a conformation where the local motion of the fluorescein is less restricted than in the DNA−GalR complex but not so mobile as in free DNA.

Since positions 12 and 19 in these oligonucleotides are at different locations relative to the pseudodyad symmetry axis, it is not surprising that the observed anisotropy changes and estimated parameters vary with labeling position. Both the strength of binding and the magnitude of the fluorescence change may vary with labeling position as well as the chemical nature of the linker arm and label. In our studies, the weaker binding oligonucleotide shows more clearly the presence of the ternary complex. This correlation is purely fortuitous. In studies on TyrR by Bailey *et al.* (*15*), the fluorescence changes observed upon DNA binding were highly sensitive to the position of label. There, the tightest binding oligonucleotide showed the greatest fluorescence change while some labeling positions showed no significant fluorescence change upon binding.

Changes in intensity and anisotropy have been interpreted assuming a direct correspondence with the binding of DNA to GalR. In principle, it is possible that the change of fluorescence intensity is due solely to the binding of GalR with the fluorophore, rather than a reflection of the binding to DNA. This possibility is eliminated since almost no change in either anisotropy or intensity is observed when GalR is mixed with labeled control DNA (Figure 4) and no intensity change is observed for F-19-O_EDNA.

Comments on Parameter Estimation from the Binding Data. In the experimental results presented here, there are two spectral responses, fluorescence intensity and anisotropy. Both of these derive from labeled DNA; thus, the only detectable chemical species are those involving DNA. This affects our ability to determine and resolve binding parameters from these data. The K_d of DNA−GalR is well-determined from single titrations since there are two spectral responses, three chemical species, and two detectable species. As more complex models are considered, the number of chemical species, spectrally detectable species, and equilibrium binding equations increases while the number of spectral responses remains constant. Thus, resolution of binding parameters for these models requires additional titration data, and the confidence intervals for these parameters are necessarily broader. Several constraints are available to aid in acceptance or rejection of specific models. First, the K_d of DNA−GalR from any appropriate model should correspond to the K_d estimated from a single titration of DNA with GalR alone. Second, the estimated K_d's for D-galactose binding to GalR should be independent of labeling position within the O_E site and should also correlate well with measurements of the same equilibrium by independent means. This tacitly assumes that only one model is appropriate and that it applies to both labeled O_EDNA constructs.

The fitted curves and reduced χ^2 from the two models indicate that the binary model is inconsistent with experimental data while the ternary model fits the data well (Table 1). Application of the criteria discussed above increases our confidence in this assignment. For both labeled oligonucleotides and both models, the K_d of DNA−GalR was comparable to that obtained from titration of DNA with GalR alone. The fitted GalR−D-galactose K_d for the ternary model is 3.3 μM using F-19-O_EDNA and 5.1 μM using F-12-O_EDNA. These compare well with each other and with the value of 5.3 μM (350 mM KCl, pH 7.3, at 25 °C) obtained using intrinsic tryptophan fluorescence (*44*). The same K_d's obtained using the binary model, however, are not self-consistent (1.9 mM using F-19-O_EDNA and 15 μM using F-12-O_EDNA), nor are they consistent with literature values. Taken together, these results suggest that the ternary model is the most appropriate model for this system.

Table 2: Fitted Anisotropy of Spectroscopically Detectable Species[a]

	F-19-O_EDNA		F-12-O_EDNA	
model and species	r	σ	r	σ
ternary model				
O_EDNA	0.039	3.0×10^{-4}	0.040	2.2×10^{-4}
O_EDNA−GalR	0.117	5.1×10^{-4}	0.086	4.3×10^{-4}
O_EDNA−GalR−D-galactose	0.112	17.8×10^{-4}	0.093	11.9×10^{-4}
O_EDNA−GalR−D-galactose$_2$	0. 092	5.3×10^{-4}	0.044	7.2×10^{-4}
binary model				
O_EDNA	0.039	3.1×10^{-4}	0.042	1.6×10^{-4}
O_EDNA−GalR	0.101	2.8×10^{-4}	0.088	3.8×10^{-4}

[a] σ represents ± one standard deviation of the estimated anisotropies.

Comparison with Other Studies. The dissociation constants (using the ternary model) for binding of F-19-O_EDNA and F-12-O_EDNA to GalR are 319 nM and 76 nM, respectively, in a buffer of 300 mM KCl, 25 mM KH_2PO_4/K_2HPO_4 (pH 7.4), 1 mM $MgCl_2$, and 0.02% (w/v) NaN_3 and at 25 °C. These values are not corrected for the small change in salt concentration due to addition of GalR dissolved in 1 M KCl. Previous studies using gel mobility shift assays have yielded various equilibrium association constants: 10^8 M^{-1} for GalR with a 22 bp O_EDNA in a buffer containing 200 mM KCl, 10 mM Tris (pH 8.0), 1 mM DTT, 0.1 mM EDTA, and 3% ficol and at 25 °C (*6*); and 1.25×10^8 M^{-1} for GalR with a 418 bp DNA containing *gal* O_E in a buffer containing 100 mM KCl, 40 mM Tris-HCl (pH 8), 10 mM $MgCl_2$,1 mM DTT, and 100 μg/mL BSA at 37 °C (*12*). The major differences in solutions between this fluorescence assay and the gel mobility shift assays include the salt concentration, buffer compositions, temperature, and the pH of the solutions. Brenowitz *et al*. (*45*) have investigated the effects of pH, salt concentration, and temperature on the binding of GalR to O_E and O_I using quantitative footprinting. Extrapolation of their data to 0.3 M KCl and interpolation to pH 7.4 yield an estimated K_d = 100 nM. This is close to the K_d that we obtain with F-12-O_EDNA. On the other hand, the K_d of F-19-O_EDNA to GalR is somewhat larger and suggests that the fluorescein attached at position 19 interferes with binding of GalR. Since the K_d for GalR binding to F-12-O_EDNA is similar to that obtained from other methods (after correction for conditions), there is no discernible interference with GalR binding due to the label at position 12.

GalR Monomer−Dimer−Tetramer Equilibria. Brenowitz *et al*. (*45*) have analyzed the binding of GalR to DNA containing either the O_E or the O_I site. To adequately fit their data, it was necessary to include a monomer−dimer equilibrium for GalR where the dimer binds DNA more strongly than the monomer. The estimated monomer−dimer dissociation constant was 2.2 nM. Experimental data from the present study were reanalyzed including the GalR monomer−dimer equilibrium as a fixed parameter with K_d = 2.2 nM. The K_d of O_EDNA-$GalR_{monomer}$ was set to 10^4-fold larger than that of O_EDNA−$GalR_{dimer}$. The K_d for $GalR_{monomer}$−D-galactose was assumed to equal that of $GalR_{dimer}$−D-galactose. In the ternary model, the dissociation constant of DNA−monomer−D-galactose is equal to that of DNA−dimer−D-galactose. No significant improvement in the fitting was obtained for either model by inclusion of the monomer−dimer equilibrium. Under our experimental conditions, the data are adequately described by GalR existing as a static dimer.

It is known that complete repression of the *gal* operon by GalR requires binding of GalR to both O_E and O_I, supercoiled DNA, and the histone-like factor HU (*11*). It has been suggested, based on analogy to the *lac*I system, that formation of a GalR tetramer−DNA complex may play a role in regulation of *gal*. In principle, the presence of a $GalR_4$−DNA_2 complex that dissociates to a $GalR_2$−DNA complex upon inducer binding would be consistent with our data. However, it is not likely that species higher than dimer are present in our studies. In early studies (*45*), no evidence was found for GalR tetramer formation alone or in combination with DNA. Hsieh *et al.* (*46*) have used analytical centrifugation to study GalR and find no evidence for species other than dimer over the concentration range of 1−7 μM. Further, GalR, a member of the *lac*I family, does not contain the domain homologous to the one known to function in tetramer formation in *lac*I. We hope to carry out time-resolved anisotropy studies which should help to further clarify this point.

Comments on Nonspecific Binding. We consider the possibility that the ternary complex detected here and in previous studies on GalR (*43*) may be the result of nonspecific interactions. The test this possibility, we have titrated GalR into labeled nonspecific DNA (Figure 4A) up to the highest concentrations used with specific O_EDNA. Essentially no change in either anisotropy or intensity was observed. Subsequent further titration of inducer (D-galactose) into the mixture of labeled nonspecific DNA and GalR (Figure 4B) also resulted in no change in anisotropy. If the ternary complex is nonspecific in nature, then one should expect the limiting anisotropies of the mixtures of all three components to be independent of sequence and site of labeling under comparable experimental conditions. Our results show that this is not the case. Thus, we believe that the ternary complex is the result of a specific interaction with altered conformation from the binary O_EDNA−GalR binary complex.

CONCLUSION

We present evidence for a ternary complex of GalR, inducer, and operator DNA that may function in the regulation of *gal* in *E. coli*. This result confirms and extends the work of Adhya and co-workers (*43*). Future dissection of the fluorescence signals observed here will provide insight into the structural changes underlying the measured anisotropy changes. In particular, we plan to carry out time-resolved anisotropy studies on this system using both labeled DNA, as reported here, and labeled GalR.

The fluorescence approach presented here can be used to study other transcription regulation systems and other biological processes which are based on the DNA−protein interactions. These solution-based fluorescence methods are aimed at circumventing some of the difficulties associated with gel mobility shift assays and related methods and providing a complementary approach with a different and unique view of these systems. The fluorescence methods have been and can be used to characterize multiple linked equilibria involved in transcription regulation systems and to obtain dynamic information under true solution equilibrium conditions. Such studies are key to understanding the mechanisms of gene control at the molecular level.

ACKNOWLEDGMENT

We thank Dr. Sankar Adhya for generously supplying plasmids and for many helpful discussions. We thank Drs. Tim Lohman, Mike Brenowitz, and Bob Schleif for critical comments and helpful discussions.

REFERENCES

1. Adhya, S. (1987) in *Escherichia coli and Salmonella: Cellular and Molecular Biology* (Neidhardt, F. C., Ed.) pp 1503−1512, American Society for Microbiology, Washington, DC.
2. Choy, H., and Adhya, S. (1996) in *Escherichia coli and Salmonella: Cellular and Molecular Biology* (Neidhardt, F. C., Ed.) pp 1287−1299, ASM Press, Washington, DC.
3. Irani, M. H., Orosz, L., and Adhya, S. (1983) *Cell 32*, 783−788.
4. Majumdar, A., and Adhya, S. (1989) *J. Mol. Biol. 208*, 217−223.
5. Majumdar, A., and Adhya, S. (1987) *J. Biol.Chem. 262*, 13258−13262.
6. Wartell, R. M., and Adhya, S. (1988) *Nucleic Acids Res. 16*, 11531−11541.
7. Adhya, S., and Miller, W. (1979) *Nature 279*, 492−494.
8. Majumdar, A., and Adhya, S. (1984) *Proc. Natl. Acad. Sci. U.S.A. 81*, 6100−6104.
9. Majumdar, A., Rudikoff, S., and Adhya, S. (1987) *J. Biol.Chem. 262*, 2326−2331.
10. Nakanishi, S., Adhya, S., Gottesman, M. E., and Pastan, I. (1973) *Proc. Natl. Acad. Sci. U.S.A. 70*, 334−338.
11. Aki, T., Choy, H. E., and Adhya, S. (1996) *Genes Cells 1*, 179−188.
12. Goodrich, J. A., and McClure, W. R. (1992) *J. Mol. Biol. 224*, 15−29.
13. Zhou, Y. N., Chatterjee, S., Roy, S., and Adhya, S. (1995) *J. Mol. Biol. 253*, 414−425.
14. Allen, D. J., Darke, P. L., and Benkovic, S. (1989) *Biochemistry 28*, 4601−4607.
15. Bailey, M., Hagmar, P., Millar, D. P., Davidson, B. E., Tong, G., Haralambidis, J., and Sawyer, W. H. (1995) *Biochemistry 34*, 15802−15812.
16. Bujalowski, W., and Lohman, T. M. (1987) *Biochemistry 26*, 3099−3106.
17. Bujalowski, W., and Jezewska, M. J. (1995) *Biochemistry 34*, 8513−8519.
18. Carver, E. T., Jr., Hochstrasser, R. A., and Millar, D. P. (1994) *Proc. Natl. Acad. Sci. U.S.A. 91*, 10670−10674.
19. Casas-Finet, J. R., and Karpel, R. L. (1993) *Biochemistry 32*, 9735−9744.
20. Guest, C. R., Hochstrasser, R. A., Dupuy, C. G., Allen, J. D., Benkovic, S. J., and Millar, D. P. (1991) *Biochemistry 30*, 8759−8770.
21. Hagmer, P., Bailey, M., Tong, G., Haralambidis, J., Sawyer, H., and Davidson, B. E. (1995) *Biochim. Biophys. Acta 1244*, 259−268.
22. Heyduk, T., and Lee, J. C. (1990) *Proc. Natl. Acad. Sci. U.S.A. 87*, 1744−1748.
23. Heyduk, T., and Lee, J. C. (1992) *Biochemistry 31*, 5165−5171.
24. Heyduk, T., Lee, J. C., Ebright, Y. W., Blatter, E. E., Zhou, Y., and Ebright, R. H. (1993) *Nature 364*, 548−549.
25. LeTilly, V., and Royer, C. A. (1993) *Biochemistry 32*, 7753−7758.
26. Perez-Howard, G. M., Weil, P. A., and Beechem, J. M. (1995) *Biochemistry 34*, 8005−8017.
27. Thömmes, P., Farr, C. L., Marton, R. F., Kaguni, L. S., and Cotterill, S. (1995) *J. Biol. Chem. 270*, 35−43.
28. Gohlke, C., Murchie, A. I. H., Lilley, D. M. J., and Clegg, R. M. (1994) *Proc. Natl. Acad. Sci. U.S.A. 91*, 11660−11664.
29. Hochstrasser, R. A., Chen, S.-M., and Millar, D. P. (1992) *Biophys. Chem. 45*, 133−141.
30. Lee, S. P., Porter, D., Chirikjian, J. G., Knutson, J. R., and Han, M. K. (1994) *Anal. Biochem. 220*, 377−383.
31. Morrison, L. E., Halder, T. C., and Stols, L. M. (1989) *Anal. Biochem. 183*, 231−244.
32. Ruth, J. L. (1991) *Oligonucleotides and Analogues*, Oxford University Press, New York.
33. Sinha, N. D., and Striepeke, S. (1991) *Oligonucleotides and Analogues*, Oxford University Press, New York.
34. Vámosi, G., Gohlke, C., and Clegg, R. M. (1996) *Biophys. J. 71*, 972−994.
35. Yang, M., Ghosh, S. S., and Millar, D. P. (1994) *Biochemistry 33*, 15329−15337.
36. Yang, M., and Millar, D. P. (1996) *Biochemistry 35*, 7959−7967.
37. Lee, S. P., Kim, H. G., Censullo, M. L., and Han, M. K. (1995) *Biochemistry 34*, 10205−10214.
38. Lee, N., Francklyn, C., and Hamilton, E. P. (1987) *Proc. Natl. Acad. Sci. U.S.A. 84*, 8814−8818.
39. Dawson, R. M. C., Elliott, D. C., Elliott, W. H., and Jones, K. M. (1986) in *Data for Biochemical Research*, pp 103−114, Oxford University Press, New York.
40. Weickert, M. L., and Adhya, S. (1992) *J. Biol. Chem. 267*, 15869−15874.
41. Toptygin, D., and Brand, L. (1995) *Anal. Biochem. 224*, 330−338.
42. Gibson, K. J., and Benkovic, S. J. (1987) *Nucleic Acids Res. 15*, 6455−6467.
43. Chatterjee, S., Zhou, Y.-N., Roy, S., and Adhya, S. (1997) *Proc. Natl. Acad. Sci. U.S.A. 94*, 2957−2962.
44. Brown, M. P., Shaikh, N., Brenowitz, M., and Brand, L. (1994) *J. Biol. Chem. 269*, 12600−12650.
45. Brenowitz, M., Jamison, E., Majumdar, A., and Adhya, S. (1990) *Biochemistry 29*, 3374−3383.
46. Hsieh, M., Hensley, P., Brenowitz, M., and Fetrow, J. S. (1994) *J. Biol. Chem. 269*, 13825−13835.

BI972004V